Wavelength-dependent sleep state manipulation using light pulses in *Pogona vitticeps*

Nitzan Albeck[1,2], Mark Shein-Idelson[1,2]

[1]School of Neurobiology, Biochemistry, and Biophysics, Tel Aviv University, Tel Aviv, Israel

[2]Sagol School of Neuroscience, Tel Aviv University, Tel Aviv, Israel

*Corresponding Author: Mark Shein-Idelson, Tel-Aviv University, email: sheinmark@tauex.tau.ac.il

Supplementary Information

Supplemental Figures:

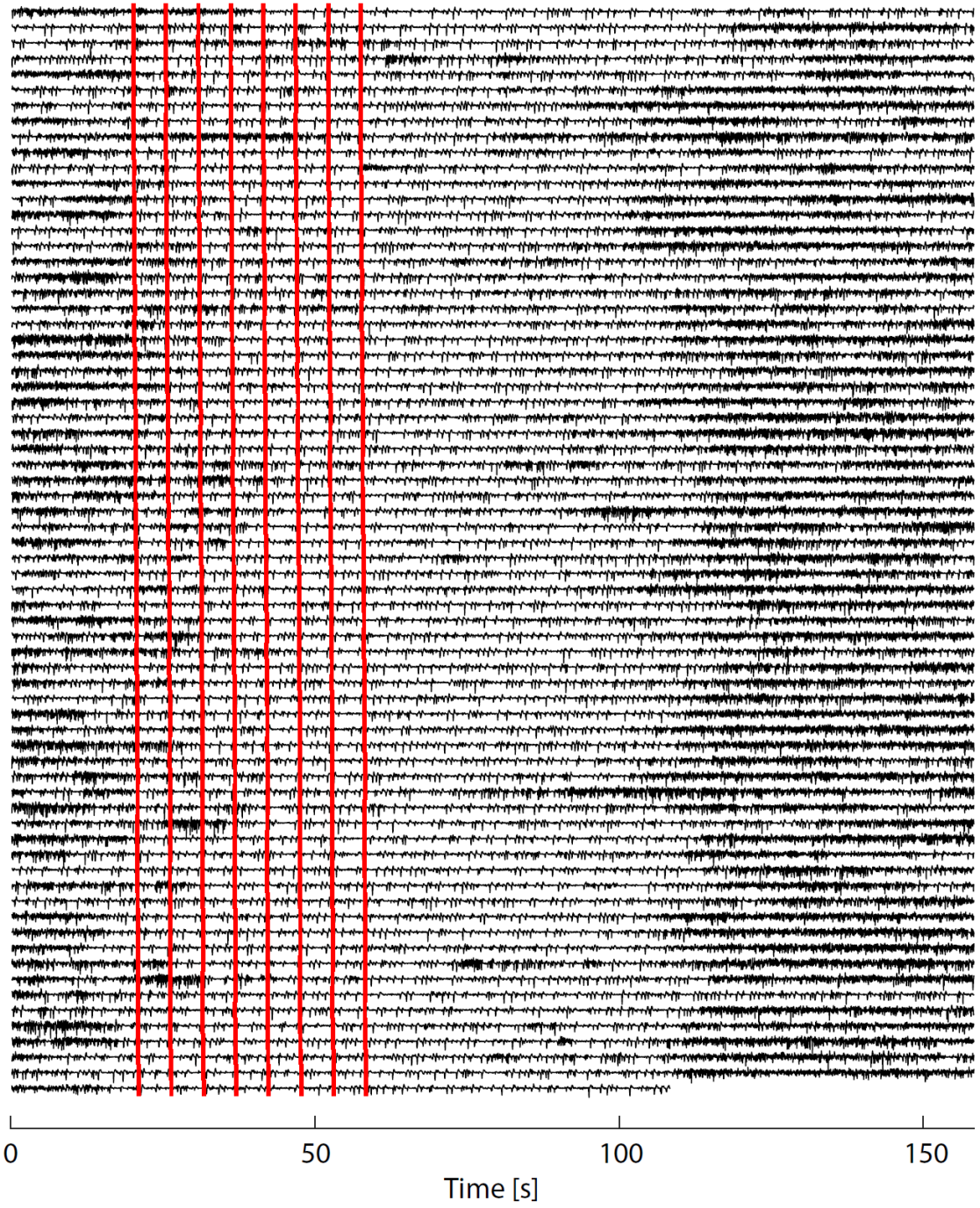

Supplementary Figure 1. Raw LFP signal across all stimulations from one night. Raw LFP trace (black) of all light stimulation trials. Time in second from left to right and top to bottom, starting from the first stimulation trial to the end of the stimulations. The night shown is one in which external white light stimulations were used.

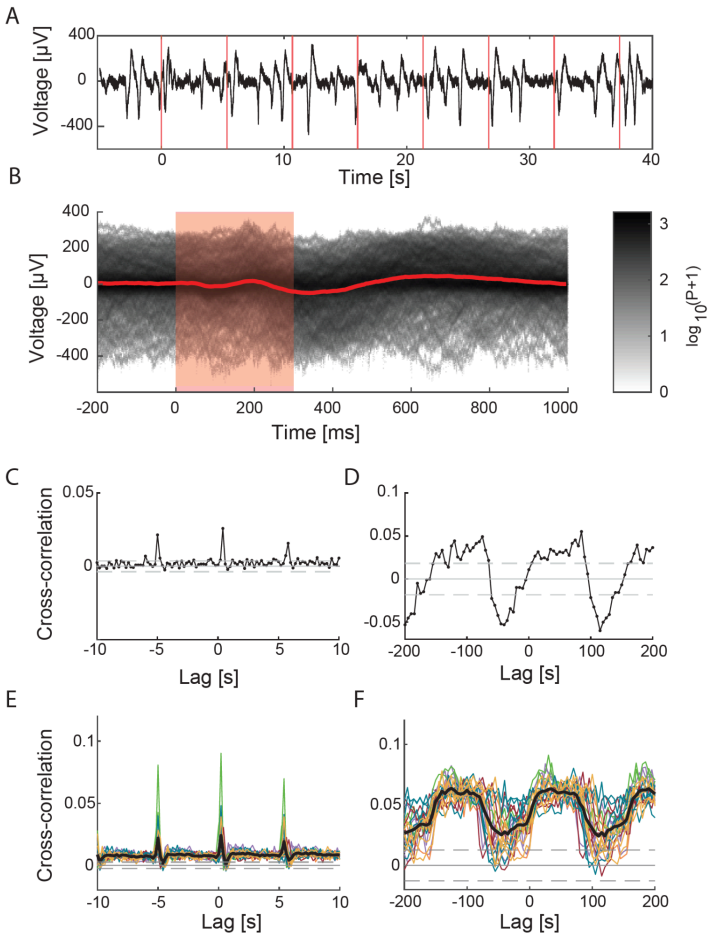

Supplementary Figure 2. Sharp waves are locked to external white light stimulations. A. Raw LFP trace (black) of one light stimulation trial (8 consecutive stimulations, red). **B.** Density plot (gray) and the average (red) of the raw traces following white light stimulation (red shade starting at t=0) over one night. **C.** Cross-correlation (200ms bins) between the binary time series of stimulation events and the binary time series of sharp wave events during one night. **D.** Long window cross-correlation (5s bins) between stimulation events and sharp wave events during one night (as in (C) but for longer lags and bins). **E. and F.** Same as (C) and (D) but for all nights (21 nights from 6 animals; white light stimulation). Color coded according to animal identity (as in Fig. 1H) with the average over nights in black. Dashed lines in (C)-(F) indicate 95% confidence bounds. We note that we observed no visible artifacts due to light stimulations. Further, such artifacts should have been tightly locked to the stimulation time (with millisecond precision). In contrast, sharp wave times were widely distributed (hundreds of milliseconds following stimulation) and were similar in shape to naturally occurring sharp waves.

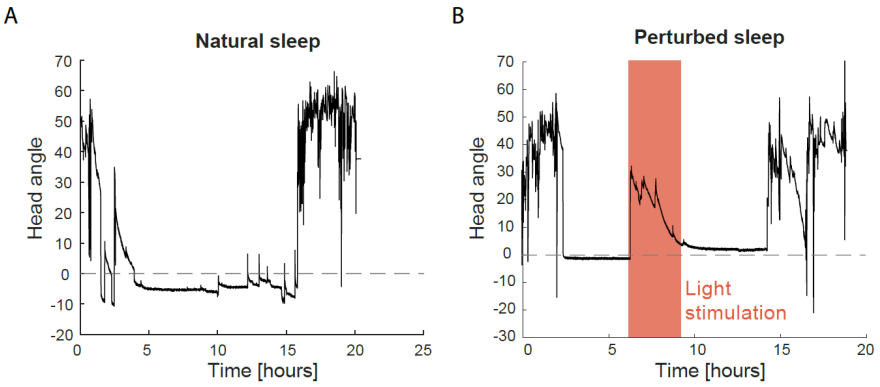

Supplementary Figure 3. Head angle dynamics throughout the night with internal red stimulation. Dynamics of head angles were approximated from the orientation of the accelerometer (Methods) during a night of natural sleep (A) and a night with internal red stimulations (red shade). Dashed grey line marks the angle at which the animal's head is rested on the ground.

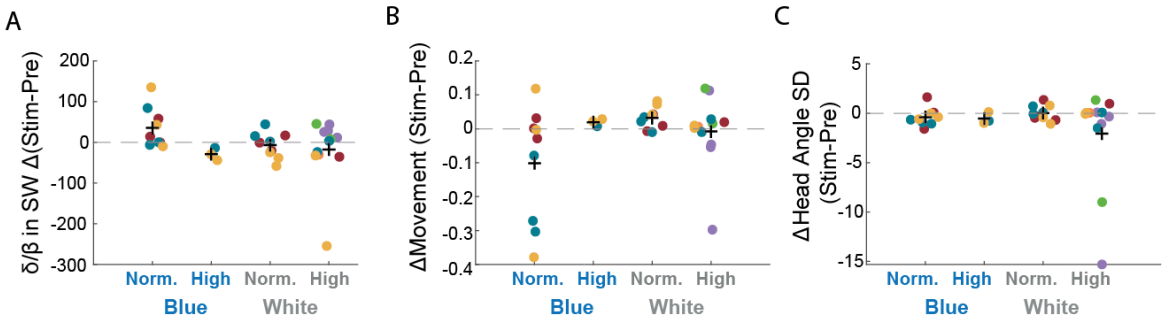

Supplementary Figure 4. Sleep is not perturbed during high intensity stimulations. A. Average δ/β power difference (Δ) between stimulation period and pre-stimulation period, averaged over all SW cycles. All groups are not significantly different from zero. **B.** Movement differences (Δ) between pre-stimulation and stimulation sleep periods were not significantly different from zero. **C.** Head angle SD differences (Δ) between pre-stimulation and stimulation periods were not significantly different than zero. In all panels, data is color-coded according to animal identity (as in Fig. 1H), with averages in Black. Wilcoxon signed-rank test was used to evaluate the difference of each group from 0. A total of (9, 3, 9, 12) nights from (3, 2, 3, 6) animals were recorded for Blue, high intensity Blue, White, and high intensity White, respectively.

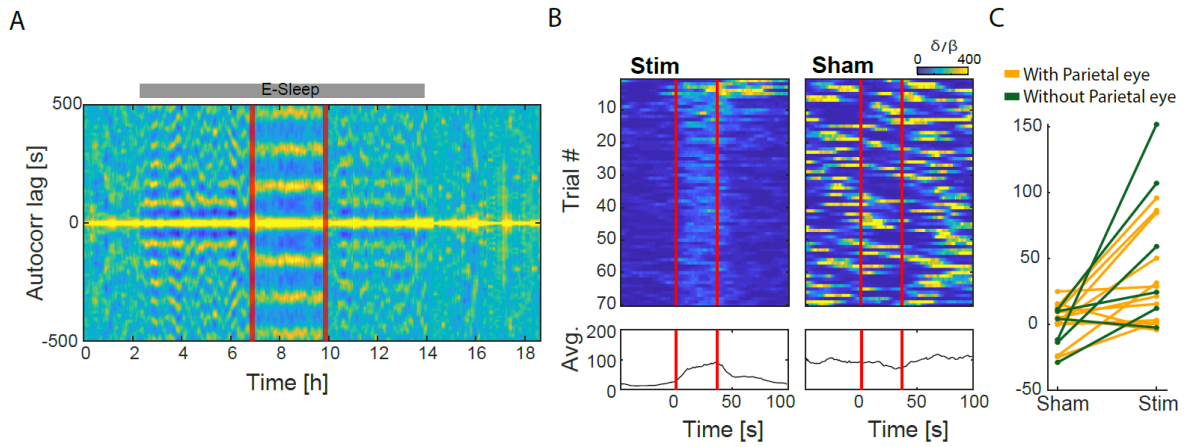

Supplementary Figure 5. Cycle entrainment persists despite parietal eye removal. A. Sleep oscillations during a light-stimulated night after parietal eye removal. The moving autocorrelation of δ/β throughout the night (as in Fig. 1I). Red lines mark stimulation onset and offset. The top gray bar is the electrophysiological sleep period. **B.** Top: δ/β ratio across all light stimulation cycles of from the night in (A) during (left) and before (right) the light stimulation period (Sham, the intervals between trials were the same as during stimulation but extracted from the natural sleep preceding the first stimulation). Bottom: δ/β averaged over all trials. Red line marks stimulation onset and offset. **C.** Difference between the average δ/β during stimulations (last 30s of the stimulation period); and before the stimulations (30s before each stimulation period), averaged across all trials for stimulations (stim) and natural sleep before stimulations (sham, as Fig. 1H). Color-coded according to the presence of the parietal eye: 13 nights before the parietal eye removal (yellow), and 6 nights after the removal (green), from 2 animals. No significant difference between the groups (p = 0.41 and 0.37 for sham and stimulation groups, respectively).

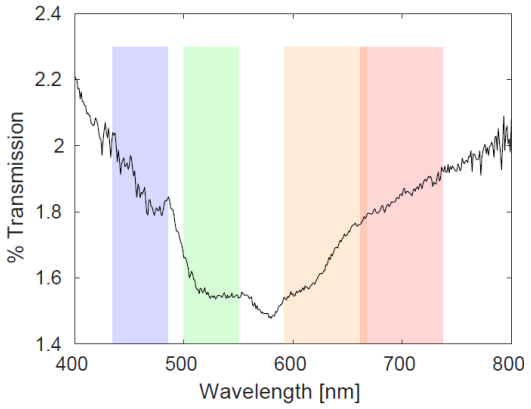

Supplementary Figure 6. Eyelid wavelength dependent transmission verification. Wavelength-dependent light transmission through the eyelid, taken using the LAMDA spectrophotometer, an example. Shades show the band-filter borders used in Fig. 3J: Blue: 435-485nm; Green: 500-550nm; Red: 592-667nm; Long Red: 662-737nm.

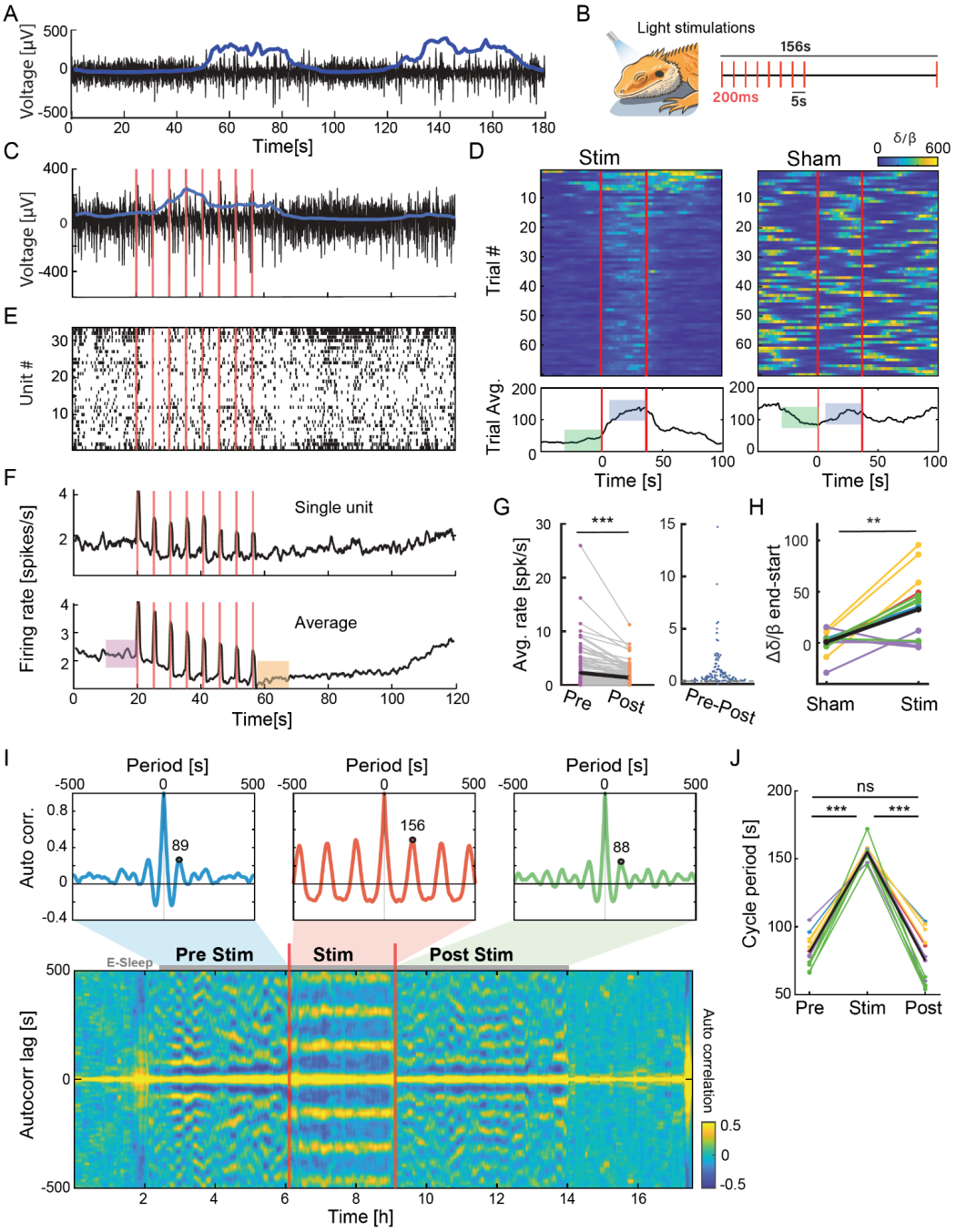

Supplementary Figure 7. Sleep states can be controlled and entrained using internal red stimulations. A. Raw electrode recording (black) from aDVR during unperturbed sleep showing state oscillations quantified by the δ/β frequency ratio (blue). **B.** Schematics of the internal light stimulation protocol. Stimulations were delivered by an optic fiber connected to the head. One cycle of the stimulation consisted of 8 light pulses (200ms each), separated by 5s intervals, followed by 120s without stimulation. 70 consecutive cycles were delivered per night. **C.** Example raw data (black) and the corresponding δ/β ratio (blue) recorded during one stimulation cycle (red lines mark individual light pulses). **D.** Top: δ/β ratio across all light stimulation cycles of one night during (left) and before (right) the light stimulation period (Sham, the intervals between trials were the same as during stimulation but extracted from the natural sleep preceding the first stimulation). Bottom: δ/β averaged over all cycles. The red line marks stimulation onset and offset. Color boxes mark the time segments used for calculating the average in (H). **E.** Raster plot of spiking activity during the stimulation cycle in (C). **F.** Average spiking rate across all stimulation cycles recorded from one neuron (top) and averaged over all neurons (bottom; 141 units, 4 nights). Notice gradual decrease during stimulation and increase after stimulations end. Color boxes mark the time segments used for calculating the averages in (G). **G.** Left: Average spiking rate before stimulation (Pre: 10s before trial onset; purple box in (F)) vs after stimulations (Post: 10s

after the last pulse within a cycle; orange box in (F)) for different units ($p=6.67*10^{-21}$, Wilcoxon, n=141 units from 4 nights in 3 animals). Right: The differences between Pre and Post across neurons. **H.** Difference between the average δ/β during stimulations (last 30s of the stimulation period; blue box in (D)) and before the stimulations (30s before each stimulation period; green box in (D)), averaged across all trials for stimulations (stim) and natural sleep before stimulations (sham) (15 nights from 5 animals, color-coded according to animal identity; black is the average over nights; p=0.008, Wilcoxon). **I.** Bottom: The moving autocorrelation of δ/β throughout the night. Red lines mark stimulation onset and offset. Top: average autocorrelation calculated before stimulation (Pre), during stimulations (Stim: 0.5-3h after first stimulation onset), and after stimulations (Post: 0.5h - sleep end). **J.** Cycle period calculated from the averaged autocorrelation before, during, and after light stimulation (as in (I)). Cycle period changed significantly during stimulations and resumed its natural time after stimulations ended (p=0.0007, 0.0007, 0.37 for Pre vs. Stim, Stim vs. Post, Pre vs. Post, respectively, Wilcoxon corrected). Animal identity color-coded as in Fig. 1H and averaged (black) over recorded nights (13 nights from 5 animals).

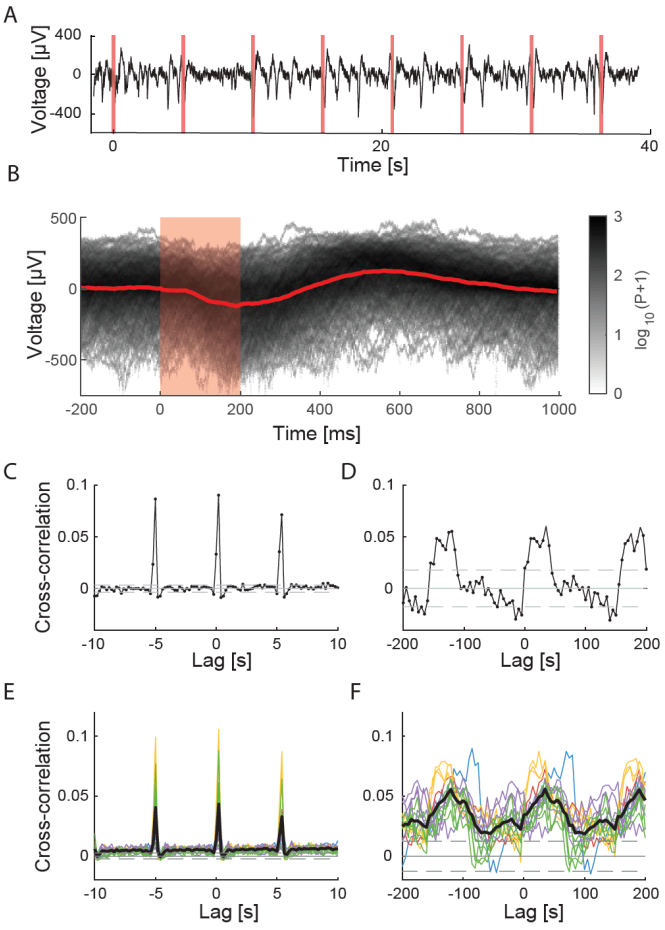

Supplementary Figure 8. Sharp Waves are locked to internal red light stimulations. A. Raw LFP trace (black) of one light stimulation trial (8 consecutive stimulations, red). **B.** Density plot (gray) and the average (red) of the raw traces following red internal light stimulation (red shade starting at t=0) over one night. **C.** Cross-correlation (200ms bins) between the binary time series of stimulation events and the binary time series of sharp wave events during one night. **D.** Long window cross-correlation (5s bins) between stimulation events and sharp wave events during one night (as in (C) but for longer lags and bins). **E. and F.** Same as (C) and (D) but for all nights (15 nights from 5 animals; 635nm wavelength stimulation). Color coded according to animal identity (as in Fig. 1H) with the average over nights in black. Dashed lines in (C)-(F) indicate 95% confidence bounds. We note that we observed no visible artifacts due to light stimulations. Further, such artifacts should have been tightly locked to the stimulation time (with millisecond precision). In contrast, sharp wave times

were widely distributed (hundreds of milliseconds following stimulation) and were similar in shape to naturally occurring sharp waves.

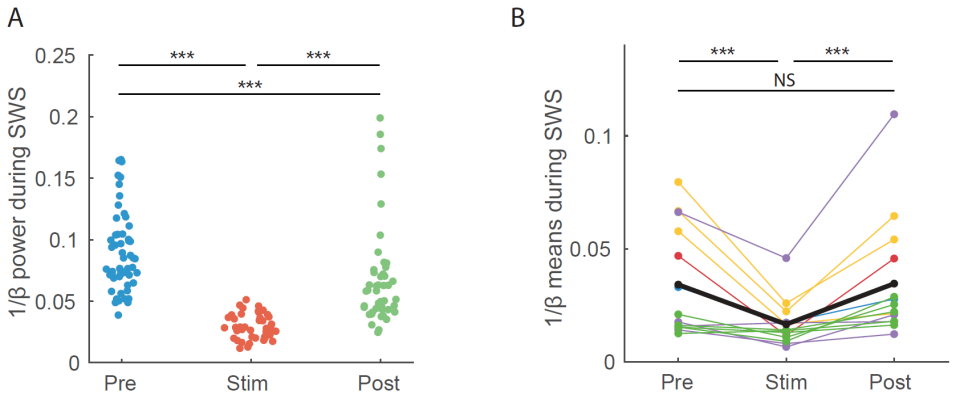

Supplementary Figure 9. 1/β activity during SW sleep. A. 1/β power during each SW sleep cycle (high δ/β) before (blue), during (red), or after (green) stimulations (same events as in Fig. 4B) ($p=1.4*10^{-16}$, $2.8*10^{-11}$, $7.8*10^{-5}$ for Pre vs. Stim, Stim vs. Post, Pre vs. Post, respectively, Mann-Whitney corrected). **B.** Average 1/β power for SW cycles for all internal red stimulation nights. 14 nights from 5 animals, color-coded as in Fig. 1H, average in black (p= 0.0018, 0.0004 for Pre vs. Stim, Stim vs. Post, Wilcoxon corrected). We note that while both 1/β and δ/β (Fig. 4B) exhibit the same entrainment profile, their intensities are quantitatively different.

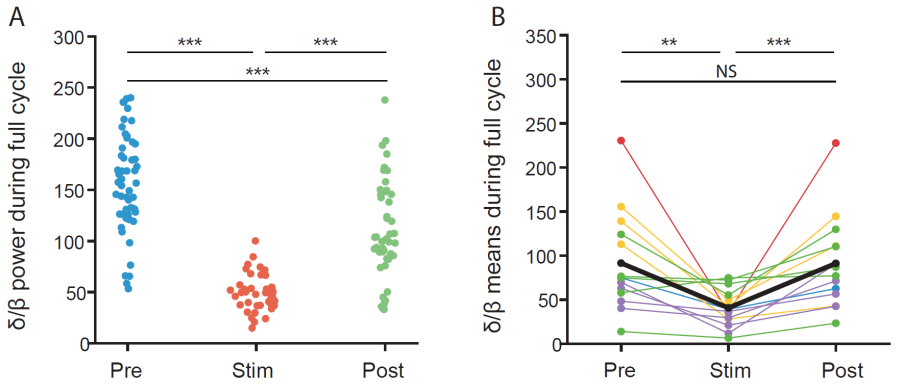

Supplementary Figure 10. δ/β power during the full cycle. A. δ/β power mean over the full SW-REM sleep cycles during pre-stimulations, stimulations, and post-stimulations night periods (same night as in Fig. 4B). ($p=1.2*10^{-15}$, $2.3*10^{-9}$, $7.1*10^{-5}$ for Pre vs. Stim, Stim vs. Post, Pre vs. Post, respectively, Mann-Whitney corrected). **B.** Average δ/β power for full SW-REM cycles for all internal red stimulation nights. 14 nights from 5 animals, color-coded according to animal identity as in Fig. 1H, average in black (p= 0.005, 0.0004 for Pre vs. Stim, Stim vs. Post, Wilcoxon corrected).

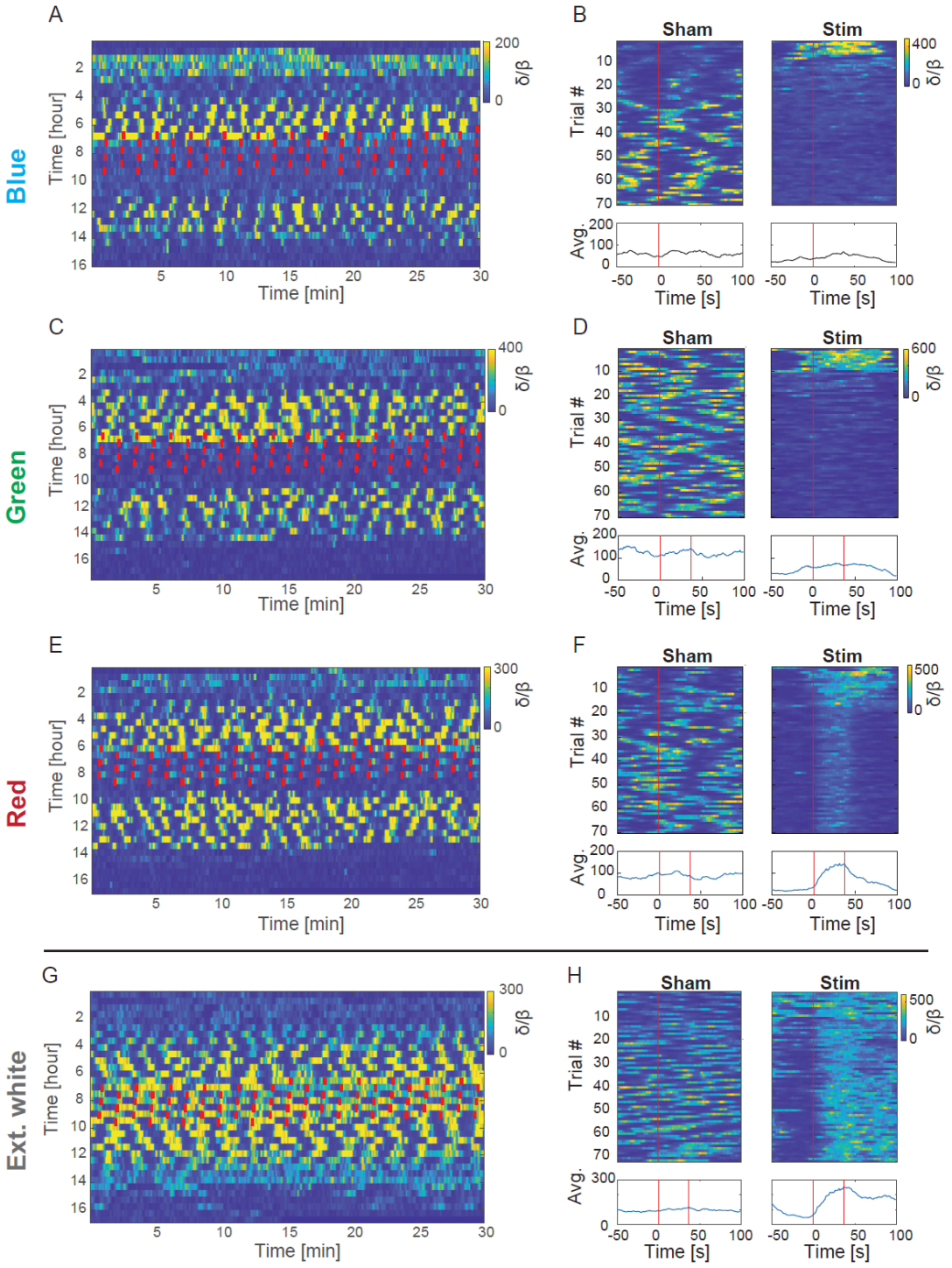

Supplementary Figure 11. Example of δ/β dynamics for different internal stimulation wavelengths. A. δ/β dynamics across all night - internal blue wavelength (473nm). The δ/β ratio is measured over 10s moving windows (1s steps) around night-time. Each horizontal row represents a 30 min segment (running left to right); successive 30 min segments run continuously from top to bottom. Stimulations trials start times in red vertical lines. **B.** Top: δ/β power across all light stimulation cycles of one night (right) and during sham stimulations performed over the sleep segment preceding light stimulations (left). Bottom: δ/β averaged over all cycles. Red line marks stimulation onset and offset. **C-D, E-F, G-H.** Same as A-B, but for internal Green wavelength (532nm) and Red wavelength (635nm), and compared to external white light, respectively. A-F were recorded from the same animal.

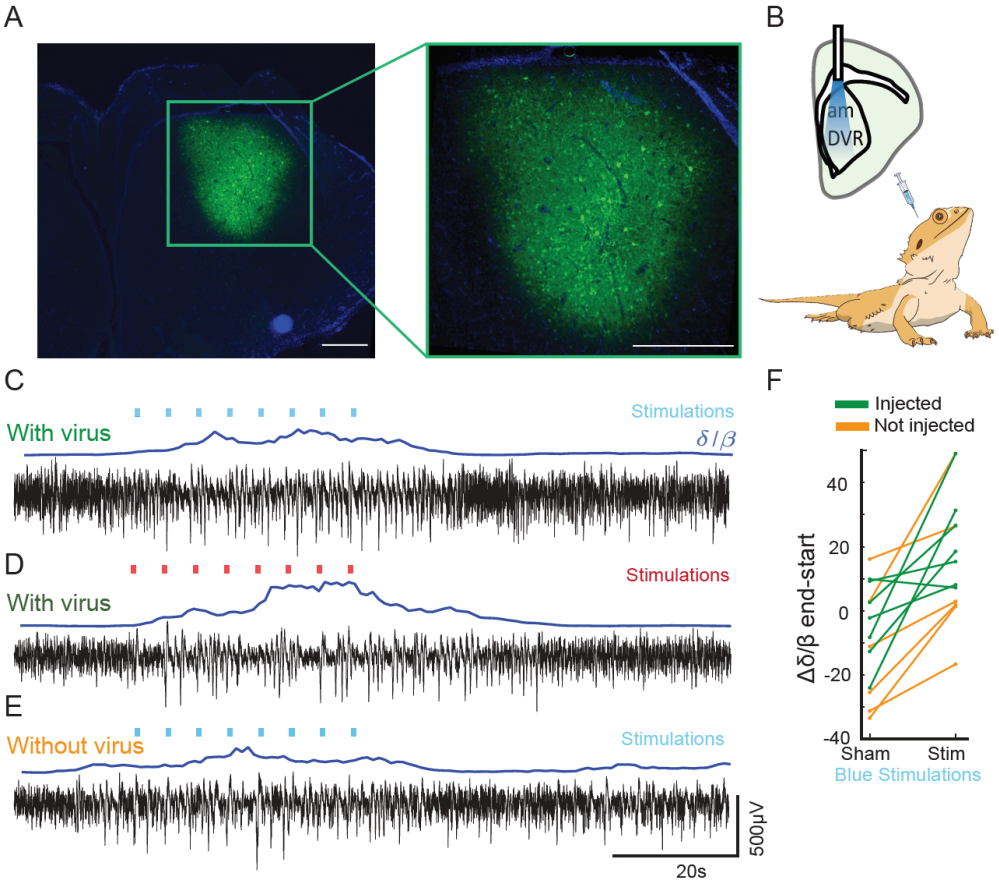

Supplementary Figure 12. Brain state changes are not the outcome of optogenetic activation but the light used for this activation. A. Fluorescence image of a brain slice stained with DAPI (blue) and GFP (green) expressed by virally infected neurons in the aDVR (scale bars, 500µm). **B.** Illustration of the experimental procedure for optogenetic experiments. AAV viruses were injected into *P. vitticeps* aDVR to express ChR2 and GFP and an optic fiber was implanted above the injected region to provide light excitation for activating ChR2 (Methods). **C.** Raw data (black) recorded during internal light stimulations (488nm, blue vertical lines), from an animal injected with viral particles. **D.** Raw data (black) during internal light stimulations (635nm, red vertical lines), from an animal injected with viral particles. **E.** Raw data (black) during internal light stimulations (488nm, blue vertical lines), from an animal not injected with viral particles. Blue traces in (C)-(D) correspond to δ/β power. **F.** Difference between the average δ/β power during light stimulations (last 30s of the stimulation period) and before stimulations (30s before each stimulation period), averaged across all trials. Notice increases during stimulations (Stim, 488nm), relative to natural sleep before stimulations (Sham) (as in Fig. 1H), for both virally injected (Green, 8 nights from 2 animals) and non-injected (Orange, 6 nights from 3 animals) animals. No statistical difference found between groups (p=0.3, 0.1 for Sham and Stim, respectively, Mann-Whitney).

Supplemental Methods

Viral injection

In two (out of 9) animals we injected viral particles expressing channelrhodopsin (ChR2) into aDVR. Injections were motivated by previous reports demonstrating sleep state manipulation by perturbing neuronal excitability using optogenetics in rodents [1]. Injections were discontinued after discovering that brain state entrainment was light induced but independent of viral vectors (Fig. S12). For the animals injected with viral particles, the craniotomy was performed as explained in Methods. AAV9-hSyn-ChR2(H134R)-mCh (Addgene,26976-AAV9) virus were injected using a stereotactic Hamilton needle (1µl, Neuros Syringe, Model 7001 KH, 32 gauge, Point Style 4, Hamilton). The needle was lowered to a depth of 1.5mm, and a micro injection pump was used to inject 200nL at a rate of 50nL/min. Five weeks after virus injection, animals underwent a second surgery during which the electrode array, reference electrode, and optic fiber were inserted (see Surgery, Methods). Viral transcription was verified using the IHC staining.

Brain Slices and IHC Staining

When the recording ended, the lizards were deeply anaesthetized with ketamine (70mg/kg) and medetomidine (2.1mg/kg). When loss of the foot-withdrawal and corneal reflexes was verified, the lizard was perfused transcardially with cold PBS followed by 4% paraformaldehyde (PFA) in PBS, according to [2]. The brain samples were post-fixed with 4% PFA–PBS for 24h at 4°C and subsequently immersed in 15% sucrose for 24h at 4°C, followed by 30% sucrose for 24h at 4°C. The brains were then submerged in O.C.T embedding medium (Fisher HealthCare, 23-730-571) and kept at -80°C. Brains were sectioned coronally (30 µm) with a cryostat (Leica CM 1950) at −18°C. IHC. The sections were washed with PBS 3 times and with 0.5% PBST (Triton-x100 0.5% in PBS) once. Then, sections were permeabilized for 1h at room temperature in a blocking solution (0.3% PBST: PBS with 0.3% Triton X-100 and 10% Normal Goat Serum (NGS, ab7481)) and incubated with primary antibodies (Rabbit anti-GFP, ab290 Abcam, 1:1000) in blocking for 1hr at 37°C. After washing with 0.1% PBST three times, the samples were incubated with secondary antibodies conjugated with appropriate fluorophore (Goat Anti-Rabbit-Alexa Fluor 488, ab150077, Abcom, 1:500) in blocking solution for 2h at room temperature, followed by three washes with 0.1% PBST. After rinsing with PBST, the samples were mounted with Fluoromount-G with DAPI (Invitrogen Cat. Num. 00-4959-52), and covered with coverslips. Images were acquired using an inverted fluorescence microscope (Olympus IX73).

Supplemental References

1. Weber F, Chung S, Beier KT, Xu M, Luo L, Dan Y. Control of REM sleep by ventral medulla GABAergic neurons. *Nature*. 2015;526(7573):435-438. doi:10.1038/nature14979

2. Hoops D. A perfusion protocol for lizards, including a method for brain removal. *MethodsX*. 2015;2:165-173. doi:10.1016/j.mex.2015.03.005